Published in final edited form as:
Ann Surg Oncol. 2008 May ; 15(5): 1414–1423. doi:10.1245/s10434-007-9778-9.

Pseudomyxoma Peritonei: Is Disease Progression Related to Microbial Agents? A Study of Bacteria, MUC2 and MUC5AC Expression in Disseminated Peritoneal Adenomucinosis and Peritoneal Mucinous Carcinomatosis

Cristina Semino-Mora[1], **Hui Liu**[1], **Thomas McAvoy**[1,2], **Carol Nieroda**[1,3], **Kimberley Studeman**[3], **Armando Sardi**[3], and **Andre Dubois**[1]

1*Laboratory of Gastrointestinal and Liver Studies, Department of Medicine, Uniformed Services University and United States Military Cancer Institute, Bethesda, MD 20814, USA*

2*University of Maryland, College Park, MD 20742, USA*

3*Mercy Health Services, Baltimore, MD 21202, USA*

Abstract

Background and Aims—Pseudomyxoma peritonei (PMP) is characterized by peritoneal tumors arising from a perforated appendiceal adenoma or adenocarcinoma, but associated entry of enteric bacteria in the peritoneum has not been considered as a cofactor. Because Gram-negative organisms can upregulate MUC2 mucin gene expression, we determined whether bacteria were detectable in PMP tissues.

Methods—*In situ* hybridization was performed on resection specimens from five control subjects with noninflamed, nonperforated, non-neoplastic appendix and 16 patients with PMP [six with disseminated peritoneal adenomucinosis (DPAM) and 10 with peritoneal mucinous carcinomatosis (PMCA)]. Specific probes were designed to recognize: (1) 16S rRNA common to multiple bacteria or specific to *H. pylori*; (2) *H. pylori cagA* virulence gene; or (3) MUC2 or MUC5AC apomucins. Specimens from one patient with PMCA were examined by ultra-structural immunohistochemistry. Bacterial density and apomucin expression were determined in four histopathological compartments (epithelia, inflammatory cells, stroma, and free mucus).

Results—Enteric bacteria were detected in all specimens. Bacterial density and MUC2 expression were significantly ($p < 0.05$) higher in PMCA than in DPAM and controls and were highest in free mucin. MUC2 was also expressed in dysplastic epithelia and in associated inflammatory cells. MUC2 expression was significantly correlated with bacterial density.

Conclusions—Multiple enteric bacteria are present in PMP, and bacterial density and MUC2 expression is highest in the malignant form of PMP. Based on these observations, we propose that the bacteria observed in PMP may play a role in the mucinous ascites and perhaps promote carcinogenesis.

Pseudomyxoma peritonei (PMP) is a rare and complex disease characterized by the presence of multifocal peritoneal and omental implants of mucus-secreting epithelial cells and dissecting

Address correspondence and reprint requests to: Andre Dubois; E-mail: adubois@usuhs.edu.

Presented in part at the Society of Surgical Oncology, Cancer Symposium. March 23-26, 2006, San Diego, California.

None of the authors have any financial and personal relationship with others that might bias their work, and potential conflicts do not exist.

gelatinous ascites.[1] PMP is found in 0.02% of laparotomies and its incidence is threefold higher in females than in males.[2,3] The consensus is that most PMP originate from a perforated appendiceal mucocele, mucinous cystadenoma, or adenocarcinoma, and histopathological criteria have been set forth to differentiate cases with rapid clinical progression from those with a protracted course.

Treatment includes a combination of cytoreductive surgery (resection of the tumor and peritoneal implants) plus intraperitoneal heated chemotherapy.[4-8] Despite aggressive cytoreduction, the disease frequently relapses and survival at 1-, 5-, and 10-year is 98%, 53%, and 32%, respectively.[9] In nonappendiceal carcinomas, overall survival at 1, 3, and 5 years is even lower at 56%, 25%, and 17%, respectively.[10] Perioperative morbidity and mortality is 30% and 12%, respectively.[8] The rate of relapse is higher in patients with adenocarcinoma, but many patients with benign appendiceal neoplasms succumb to the disease after a prolonged clinical course.[11] The cause of death is recurrent mucoid ascites, proliferation of gelatinous mucin, mechanical compression of abdominal organs, increased abdominal cavity pressure, and concurrent effects on thoracic and vascular compartments.

A consistent hallmark of PMP is the presence of two specific apomucins that have the physicochemical property of a gel state: MUC2 and MUC5AC. In the normal gastrointestinal tract, MUC2 is present in intestinal goblet cells while MUC5AC predominates in stomach mucus cells. In the pre-cancerous gastric mucosa (intestinal metaplasia) and in gastric cancer, MUC2 replaces MUC5AC, being present in cellular membranes and in the pericellular ground substance.[12] Similarly, specific overexpression of MUC2 compared to MUC5AC was reported in the same locations in PMP of unknown and appendiceal (intestinal) origin.[13] It has been proposed that MUC2 is a specific and reliable molecular marker for the disease,[6,13,14] but the cause of MUC2 overexpression is unknown.

In vitro experiments have shown that the MUC2 mucin gene can be upregulated by lipopolysaccharides of Gram-negative organisms,[15,16] but we found no previous report of the presence of bacteria in PMP lesions. Since PMP is believed to result from the rupture of an appendiceal tumor into the peritoneum and the disease may present as acute appendicitis,[17,18] it is possible that enteric bacteria may spread to the peritoneum. Therefore, we investigated whether bacteria can be detected in PMP tissues and determined the level of apomucin expression in the same specimens.

MATERIALS AND METHODS

Patients

The study included archived specimens from 16 patients with the diagnosis of PMP and five patients with noninflamed, nonperforated, non-neoplastic appendices (NNA) resected at the time of gynecologic procedures. NNA specimens were considered to represent controls for normal uninfected peritoneum, intestinal flora and MUC expression. The PMP patients underwent cytoreductive surgery, i.e., peritonectomy with gastrointestinal tract resection as needed to achieve complete or near-complete elimination of PMP tissues. Resection was followed by intraoperative hyperthermic chemotherapy using 40 mg of mitomycin-C in 2-3 L of perfusate. The temperature within the abdominal cavity was maintained between 40°C and 42°C. Specimens used for the present study were 21 archived paraffin blocks of tissue obtained before intestinal resection and, in the case of PMP specimens, before the hyperthermic chemotherapy administration. At the time of cytoreductive surgery, none of the 16 patients had signs of intra-abdominal sepsis (abdominal tenderness, fever, increased white blood cells count) or evidence of intestinal perforation. The studies were approved by the institutional review boards of the participating institutions

Histopathology

Patients with PMP were classified in two groups based on histopathological criteria (ratio of epithelial cells to mucin, epithelial characteristics, atypia, mitotic rate) as described by Ronnett et al.[19] These criteria were used to characterize patients into either the prognostically more favorable category of disseminated peritoneal adenomucinosis (DPAM; $N = 6$) or the more malignant peritoneal mucinous carcinomatosis (PMCA; $N = 10$). Investigators were blinded to the histopathological diagnoses (i.e., DPAM and PMCA) when analyzing patient specimens.

In situ hybridization (ISH) studies

Specific DNA probes were designed as follows: (1) probe that hybridizes to a *16S rRNA* sequence conserved among 19,973 typed and nonculturable bacteria (TNCB) (including *C. jejuni*, *E. coli*, *S. enterica*, and the commensal *E. faecalis*), but not to human sequences published on the NCBI web site: (5′-AGCAAA CAG GAT TAG ATA CCC TGG TAG TCC AC-3′); (2) probes specific for *H. pylori 16S rRNA* (5′-ATT TCA CAC CTG ACT GAC TAT CCC GCC TAC GCG-3′) and its virulence factor *cagA* (5′-CTG CAA AAG ATT GTT TGG CAG A-3′);[20] and (3) probes specific for human *MUC2* (5′-TCC AAT GGG AAC ATC AGG ATA CAT GGT GGC-3′) and MUC5AC (5′-AGG TGT TGA AGA AGG CCG CAG CGG TGG C-3′).[12] In initial experiments, we used both cRNA and cDNA probes concurrently, and confirmed earlier observations that the two probes can detect the same structures.[12] In addition, we observed (see controls, below) that detection was abolished by RNase, but not DNase, further demonstrating that these probes were specifically targeting mRNA and that the amount of genomic DNA was undetectable. We considered that the cDNA antisense probes could be used in our system and discontinued the use of RNA probes, because they are more susceptible to degradation during storage and handling and also costlier. As an additional control, we routinely included RNase and DNase controls with each run.

Formalin-fixed tissue blocks were sectioned (5 μm) and analyzed as described.[12] In brief, each unstained section was deparaffinized, prehybridized, layered with denatured probe solution, incubated for 18 h, and washed five times with saline citrate solution to remove the unbound probe. Gene expression was detected by incubation for 2 h with anti-digoxigenin antibody-conjugated or streptavidin-conjugated alkaline phosphatase (Roche Diagnostic, Indianapolis, IN) (1:500 dilution in blocking immuno-Tris buffer). After washing, bound alkaline phosphatase was detected by covering the slides with a chromogenic substrate (nitro-blue-tetrazolium, NBT/BCIP kit; Vector Labs, Burlingame, CA), counterstaining with Nuclear Fast Red, dehydration, clearing in xy-lene, air drying and mounting with permount. *H. pylori* 16S rRNA was detected using Biotin-AP and is visible in blue. Serial sections were also processed and viewed under bright light as follows: first section: detection of *H. pylori 16S rRNA* (blue); second section: dual reaction for TNCB *16S rRNA* [blue if biotin-AP or red if digoxigenin-AP-red substrate kit (Vector) or brown if digoxigenin-peroxidase-3′,3-diaminobenzidine (DAB)].

For the fluorescence in situ hybridization (FISH) dual method, the hybridization mixture contained both a biotin-labeled probe recognizing *H. pylori 16S rRNA or MUC5AC* and a digoxigenin-labeled probe recognizing *cagA* or *MUC2*. After incubation as described above, the slides were covered with the following three layers:[12] first layer: 1 μL avidin-Texas red + 1.5 μL mouse monoclonal anti-digoxigenin; second layer: 10 μL biotin-anti-avidin + 1 μL rabbit anti-mouse-IgG-fluorescein isothiocyanate (FITC) conjugated; third layer: 1 μL avidin-Texas red + 10 μL monoclonal anti-rabbit-FITC conjugated. All antibodies were prepared in 1 mL of blocking solution. After each antibody layer, slides were incubated for 30 min at 37° C in a humid chamber and washed three times for 5 min each. After air-drying, the sections were mounted in Vectashield (Vector Labs, Burlingame, CA).

Control for nonspecific binding included:[12] (1) sense probe instead of antisense probe; (2) hybridization buffer instead of the antisense probe; (3) unlabeled antisense probe; (4) digoxigenin or biotin-labeled probe for a sequence completely unrelated to man and prokaryotes, the scorpion *Buthus martensi* Karsch neurotoxin sequence [5′-GGC CAC GCG TCG ACT AGT AC-3′];[21] (5) RNase A pretreatment (Roche); (6) DNase I pretreatment (Roche); and (7) RNase + DNase I pretreatment.

Morphometric Analysis[12]

Tissues were analyzed randomly and blindly regardless of category. The number of bacterial clusters expressing mRNA was quantified at 400× magnification in three randomly selected fields of view according to a modification of the point-counting stereological method and using an intraocular reticle of 27-mm diameter, covering 3578 μm^2 (i.e., 17,892 μm^3 for 5-μm-thick sections; Kr409, Klarman Rulings).[12] All data were expressed as mean ± standard error on the mean (SEM) number of bacteria per 10^6 μm^3 (representing an imaginary cube with sides of 100 μm or 0.1 mm). MUC2 and MUC5AC expression was determined as the volumetric density of apomucin ($Vvi/10^4 \mu m^3$). Counts were made in four selected histopathological compartments: (1) abnormal neoplastic epithelia, (2) inflammatory cells, (3) stroma (including blood vessels), and (4) free mucoid (present only in PMP). An Eclipse E 800 Nikon microscope and a digital camera (QCapture, Micropublisher 5.0, Burnaby, BC, Canada) were used for analysis and reproduction, respectively.

Transmission Electron Microscopy

Surgical specimens measuring 3 × 3 mm from one patient with PMCA were fixed overnight at 4°C in 2.5% glutaraldehyde in 0.1 M phosphate buffered saline (PBS) pH 7.3, post-fixed for 1 h at 4°C in 1% OsO4, and dehydrated in a graded series of increasing ethanol concentrations and embedded at 70°C for 12 h in Spurr low-viscosity epoxy in flat molds. Semithin 0.5 μm sections were stained with 1% toluidine blue. Thin sections (500-700 Å) were kept on square mesh nickel (300 mesh), thin bar, high-definition grids, and subjected to post-embedding immunogold reaction.[22-24]

Immunogold—For antigen retrieval (antigen unmasking), grids were incubated in a humid chamber with a saturated aqueous solution of sodium metaperiodate, 1 h at RT, followed by heating on 0.01 M sodium citrate pH 6.0 for 10 min at 95°C.[25] Sections were then washed and incubated for 30 min at RT with a blocking solution of 1% bovine serum albumin (BSA) in 0.1M phosphate buffer saline (PBS), with 0.05% Tween 20. Sections were then incubated for 90 min at RT with *H. pylori*-rabbit polyclonal first antibody (NeoMarkers, Fremont, CA), diluted at 1:500, followed by 2 h incubation at RT with a second 18 nm colloidal gold-affinity pure goat anti-rabbit IgG (H + L) antibody (Jackson ImmunoResearch, West Grove, PA), diluted 1:25 in deionized diethylpyrocarbonate (DEPC)-treated water. After washing, sections were stained with uranyl acetate in distilled water for 20 min. Control of method was performed using PBS instead of the first antibody. Sections were analyzed in a Philips CM100 transmission electron microscope at 80 kV (Biomedical Instrumentation Center, USUHS) and images were captured using a Spot Insight, monochrome digital 4 MP camera (Diagnostic Instruments, Inc., Sterling Heights, MI).

Statistical Analysis

Statistical significance was determined using one-way analysis of variance, followed by Tukey's post hoc tests to compare NNA versus DPAM versus PMCA in each cell of the tables. For example, for TNCB in epithelia, there were three comparisons: NNA versus DPAM, NNA versus PMCA, and DPAM versus PMCA. For the regression analysis, Bonferroni adjustment

to the *p*-values associated with correlation coefficients was performed. Values were expressed as mean ± SEM.

RESULTS

Histopathology

In the non-neoplastic, nonperforated mucosae of control patients, secretory mucus epithelial cells contained mucigen granules that emerged as mucus in the glandular lumen through exocytosis. Only a small amount of luminal mucus was visible, close to the apical part of the cells. The submucosa was composed exclusively of large lymphoid aggregates with a few neutrophils.

Six of the PMP patients had histological features of DPAM, characterized by peritoneal lesions composed of thick, dense, and abundant extracellular mucin and scant, simple to focally proliferative, mucinous epithelium with little cytological atypia or mitotic activity, with or without associated appendiceal mucinous adenoma.

Ten patients met histopathological criteria for PMCA, which was characterized by peritoneal lesions composed of more abundant mucus and mucinous epithelium with the architectural and cytological features of carcinoma, presence of goblet cell, infiltrating neoplastic pleomorphic cells, and adherent abnormal cells within desmoplastic stroma.

DPAM specimens were characterized by the presence of (1) multilobulated polypoid gelatinous masses lined by mucus-secreting epithelial cells and containing vessels and associated erythrocytes (Fig. 1A); and (2) inflammatory cells including neutrophils, lymphocytes, plasma cells and macrophages (Fig. 1C). PMCA was characterized by the presence of invasive adenocarcinoma (Fig. 2A) with signet ring cells, and glands lined by mucus-secreting goblet cells (Fig. 1B), in addition to more abundant gelatinous masses. In specimens of both groups, there was also accumulation of adipose tissue consisting of adipocytes with a large fat droplet occupying most of the cytoplasm and displacing the nucleus to one side of the cell.

Bacterial infection by in situ hybridization (ISH) and FISH (Figs. 2 and 3A-G)

In the non-neoplastic appendix, the *16S rRNA* of TNCB was expressed in the superficial mucus, inside epithelial and inflammatory cells, and in the lamina propria, but not in the peritoneal surface of the appendix. *H. pylori* was detected in only two of the five patients, and bacterial density was very low in those two patients.

In DPAM, *16S rRNA* was detected inside epithelial cells including goblet cells, in dilated capillaries between smooth muscle cells in the network of the connective tissue of the tunica media (Fig. 2C, TNCB, arrow), between erythrocytes (insert of Fig. 2C, TNCB), and associated with inflammatory cells. *H. pylori* was detected in all patients, but the density was lower than for TNCB. The density of the bacteria was not significantly different in DPAM versus non-neoplastic appendix specimens (Table 1).

In peritoneal mucinous carcinomatosis (PMCA), *16S rRNA* of TNCB was detected (Fig. 2A, solid arrow) in close association with malignant signet ring cells (Fig. 2A, dashed arrow pointing at two signet cells), in lymphoid aggregates, inside goblet cells (Fig. 2B, TNCB, arrow), attached to stromal cells (Fig. 2D), and in the lumen of capillaries. *H. pylori 16S rRNA* was particularly high in the free apomucin (Fig. 3A), in the cytoplasm of columnar mucus-secreting cells (Fig. 3B), inside goblet cells (Fig. 3C), and in the lumen of capillaries (Fig. 3D). When compared to NNA, PMCA specimens had a higher TNCB density in all regions (Table 1; $p < 0.05$). When compared to DPAM, however, TNCB density was significantly higher only in lymphoid aggregates and in the stroma (Table 1; $p < 0.05$). *H.*

pylori density was higher in PMCA than in NNA and DPAM only in the epithelial cells (Table 1; $p < 0.05$).

By FISH, *H. pylori 16S rRNA* and virulence factor *cagA* were coexpressed by 81% of the bacteria on the apical membrane and in the cytoplasm of malignant epithelium (Fig. 3E-G).

Transmission Electron Microscopy (Fig. 4)

Pools of mucin with floating islands of malignant epithelium were observed dissecting through the desmoplastic muscularis propria in the specimens from a patient with PMCA. In addition, columnar epithelial cells were mixed with luminal bacterial aggregates of diverse shapes. Some of the bacteria measured 2.5-3 μm in diameter and were identified as *H. pylori* by labeling with specific *anti-H. pylori* polyclonal antibody and immunogold (Fig. 4C). Bacteria were clustered in the extracellular matrix of connective tissue close to epithelial cells, embedded in ground substance or surrounded by bundles of collagen. Immunogold reaction showed groups of particles mostly in the bacterial cytoplasm and in smaller amount on flagellae.

Mucin Expression (Fig. 3H-J)

In NNA, MUC2 expression was low and mostly limited to inflammatory cells of the lymphoid aggregates whereas MUC5AC expression was high and localized to the cytoplasm of epithelial mucus secretory cells.

In DPAM, MUC2 expression was high in the mucigen granules of goblet cells, in the striated luminal surface (brush border) of absorptive intestinal cells, and in the free mucin. MUC2 expression was low in lymphoid aggregates and the stroma, and was absent from the mucus pools in areas of mucus accumulation. MUC5AC was highly expressed in the lymphoid aggregates, especially in the dense connective tissue surrounding inflammatory and smooth-muscle cells as well as collagen-rich areas surrounding fibroblasts, in the cytoplasm of inflammatory and epithelial cells, and in the stroma. When compared to the NNA specimens, MUC5AC expression was significantly lower in the epithelia and higher in the lymphoid aggregates ($p < 0.05$; Table 2).

In PMCA, strong MUC2 expression was observed in free mucin, epithelial and inflammatory cells of the lymphoid aggregates, and connective tissue surrounding vessels of the stroma. MUC5AC expression was lower and localized to inflammatory cells, although small amounts were also seen in the epithelial cells, the stroma, and the basal lamina surrounding the mucin accumulations. When compared to the NNA epithelia, MUC2 expression was higher in all the tissues and MUC5AC was lower in the epithelia and stroma and was higher in the lymphoid aggregates ($p < 0.05$; Table 2). In addition, MUC2 expression was higher compared to DPAM specimens in lymphoid aggregates and the stroma ($p < 0.05$; Table 2).

MUC2 expression was significantly ($p < 0.05$) and directly correlated with the density of TNCB *16S rRNA* in the epithelium, and with the density of *H. pylori* 16S rRNA in the epithelium, lymphoid aggregates, and free mucin. There was no significant correlation between MUC2 and MUC5AC expression or between MUC5AC expression and bacterial density.

DISCUSSION

The present observations demonstrate that enteric bacteria were present in PMP neoplastic specimens in which high levels of MUC2 expression were concurrently observed. Histochemistry and *in situ* hybridization demonstrated the presence of bacteria in PMP mucoid accumulations, neoplastic epithelia (including signet-ring cells that express intracellular mucin as shown in Fig. 2A), and lymphoid aggregates. In addition, enteric bacteria were present within PMP capillaries, in close proximity to endothelial cells and erythrocytes (Fig. 2C), similar to

the recent observations that *H. pylori* can be detected in the capillaries of the gastric mucosa.[26,27] Even though immunogold electron microscopy was performed in only one case, the demonstration of the presence of *H. pylori* by this exquisitely sensitive and precise method strongly supports the present findings.

MUC2 was detected in most specimens but the distribution depended on the disease. In DPAM, high expression of MUC2 was observed in the mucigen granules of goblet cells, in the striated luminal surface (brush border) of absorptive intestinal cells, and in the free mucin, but was low in lymphoid aggregates and the stroma, and was absent from the pools of mucus. In PMCA, in contrast, MUC2 was expressed in free mucin, in epithelial cells (in the mucigen granules of goblet cells and in the brush border of absorptive intestinal cells), in inflammatory cells of the lymphoid aggregates, and in connective tissue surrounding vessels of the stroma.

The pathophysiological significance of these observations is unclear, but it is important to note that bacterial densities and MUC2 expression were markedly elevated in the most malignant form of the disease, i.e., PMCA, reaching approximately 400 TNCB per 10^{-9} cm^3 (a cube with 0.001 cm sides). These bacteria may be commensal organisms since a lower density of similar bacteria was detected within the mucosa and submucosa of the non-neoplastic appendix. However, no such bacteria were detected on the peritoneal side of the appendices resected “in passing” during gynecological operations and the peritoneum is a tissue that is not expected to be colonized by intestinal bacteria. Thus, there were 3-6 times more bacteria, 4-30 times more MUC2, and 4-6 times less MUC5AC in PMCA than in non-neoplastic appendiceal epithelia. In lymphoid aggregates, the relative increase in MUC2 expression was less important, and MUC5AC expression was increased in PMP compared to the non-neoplastic appendix. MUC2 expression was significantly correlated with the density of enteric bacteria. However, the present observations do not provide an explanation for the stable equilibrium apparently reached between the immune system of PMP patients and the infecting bacteria. Indeed, the presence of bacteria in the peritoneum usually evolves to localized or diffuse peritonitis and associated fever, whereas no abscesses were noted in the PMP patients, and additional experiments will be required to clarify the phenomenon.

Specific detection of *H. pylori* in PMP specimens by light and ultrastructural methods was not expected, although *H. pylori* DNA was previously identified in the intestine[28] and in the stools.[29,30] In addition, the validity of the results was verified by performing multiple positive and negative controls and the experiments were repeated to confirm our observations as well as the reproducibility of the findings. Furthermore, *H. pylori* was observed in only two of the five appendiceal mucosae studied, thus suggesting that there was no consistent methodological error or contamination. Interestingly, *H. pylori* infection increases gastric mucus secretion in mice.[31] Furthermore, the observation of a significant correlation between expression of MUC2 and *H. pylori* 16S rRNA and *cagA* is similar to the earlier finding that MUC2 expression is directly correlated with *H. pylori* density in precancerous gastric metaplasia and gastric cancer.[12]

study.

Correlation between MUC2 expression of both TNCB and *H. pylori* densities is compatible with the hypothesis that bacteria play a role in mucin hypersecretion, but a cause and effect is of course not implied by the observation. Importantly, however, cytokines and lipid inflammatory mediators have been shown to increase MUC2 secretion in epithelial cell lines.[32,33] Similarly, the lipopolysaccharide (LPS) of *P. aeruginosa* as well as the culture supernatant of various Gram-negative and Gram-positive bacteria can upregulate transcription of the MUC2 gene in cell lines and in cultured human bronchial explants derived from patients with cystic fibrosis.[15,16] *P. aerugninosa* is one of the bacteria detected by the TNCB probe

used in the present It is therefore tempting to hypothesize that a similar mechanism is triggered by some of the TNCB present in PMP. In fact, the efficacy of intraperitoneal chemotherapy delivered at the time of the cytoreductive surgery may be related in part to the antibiotic activity of mitomycin. We recently observed that in vitro growth of *H. pylori* was suppressed by mitomycin at concentrations of 0.05 mg/mL (Liu and Dubois, unpublished), which is similar to the concentration used for chemotherapy. Finally, case reports have shown that administration of antibiotics[34] or of an immunomodulator[35] following surgery improved the long-term survival of patients with PMP.

The present observation that bacterial density is higher in the more malignant form of PMP does not prove that the infection plays a role in PMP carcinogenesis. However, *H. pylori* is now an accepted type I carcinogen,[36] and chronic inflammation in response to a subset of luminal bacteria is believed to lead to carcinogenesis in inflammatory bowel disease.[37,38] In addition, one of the enterobacteria recognized by the TNCB probe used in the present study, *E. faecalis*, is associated with development of rectal dysplasia and adenocarcinoma in an interleukin-10 knockout mouse model.[39] Finally, recent in vitro experiments have demonstrated that *E. faecalis* can upregulate cyclooxygenase-2 (COX-2) expression, promote chromosomal instability, and play a role in colonic carcinogenesis.[40] Interestingly, COX-2 is highly expressed in neoplastic mucinous epithelium of PMCA and DPAM, but only low expression is observed in patients with appendiceal mucinous neoplasms without peritoneal dissemination.[41] Therefore, one can hypothesize that the malignancy of PMP is promoted by the persistent presence of multiple bacteria and intense inflammation in the peritoneum, an organ expected to be sterile.

In summary, we propose that bacterial agents may have a role in the clinical syndrome of mucinous ascites characterizing PMP and hypothesize that perioperative antibiotic treatment may enhance the efficacy of cytoreductive surgery. A pilot prospective open-label study has been initiated to explore the effect of antibiotic administration before and after cytoreductive surgery on the short term and long term outcome of the disease.

ACKNOWLEDGMENTS

Supported in part by National Institutes of Health grant CA82312, USUHS grant HU83KT funded by an unrestricted gift in memory of Jessie McAvoy, and the E. Allen Davis Memorial fund. This paper is dedicated to the memory of Jessie McAvoy.

REFERENCES

1. Bradley RF, Stewart JH, Russell GB, et al. Pseudomyxoma peritonei of appendiceal origin: a clinicopathologic analysis of 101 patients uniformly treated at a single institution, with literature review. Am J Surg Pathol 2006;30:551–9. [PubMed: 16699309]
2. Mann WJ Jr. Wagner J, Chumas J, et al. The management of pseudomyxoma peritonei. Cancer 1990;66:1636–40. [PubMed: 2208015]
3. Aho AJ, Heinonen R, Lauren P. Benign and malignant mucocele of the appendix. Histological types and prognosis. Acta Chir Scand 1973;139:392–400. [PubMed: 4718184]
4. Witkamp AJ, de Bree E, Kaag MM, van Slooten GW, van CF, Zoetmulder FA. Extensive surgical cytoreduction and intraoperative hyperthermic intraperitoneal chemotherapy in patients with pseudomyxoma peritonei. Br J Surg 2001;88:458–63. [PubMed: 11260116]
5. Galani E, Marx GM, Steer CB, et al. Pseudomyxoma peritonei: the ‘controversial’ disease. Int J Gynecol Cancer 2003;13:413–8. [PubMed: 12911716]
6. Loungnarath R, Causeret S, Bossard N, et al. Cytoreductive surgery with intraperitoneal chemohyperthermia for the treatment of pseudomyxoma peritonei: a prospective study. Dis Colon Rectum 2005;48:1372–9. [PubMed: 15909071]

7. Loungnarath R, Causeret S, Brigand C, et al. [Pseudomyxoma peritonei: new concept and new therapeutic approach]. Ann Chir 2005;130:63–9. [PubMed: 15737316]
8. Levine EA, Stewart JH, Russell GB, et al. Cytoreductive surgery and intraperitoneal hyperthermic chemotherapy for peritoneal surface malignancy: experience with 501 procedures. J Am Coll Surg 2007;204:943–53. [PubMed: 17481516]
9. Gough DB, Donohue JH, Schutt AJ, et al. Pseudomyxoma peritonei. Long-term patient survival with an aggressive regional approach. Ann Surg 1994;219:112–9. [PubMed: 8129481]
10. Shen P, Hawksworth J, Lovato J, et al. Cytoreductive surgery and intraperitoneal hyperthermic chemotherapy with mitomycin C for peritoneal carcinomatosis from nonappendiceal colorectal carcinoma. Ann Surg Oncol 2004;11:178–86. [PubMed: 14761921]
11. Yan H, Pestieau SR, Shmookler BM, et al. Histopathologic analysis in 46 patients with pseudomyxoma peritonei syndrome: failure versus success with a second-look operation. Mod Pathol 2001;14:164–71. [PubMed: 11266521]
12. Semino-Mora C, Doi SQ, Marty A, et al. Intracellular and interstitial expression of H. pylori virulence genes in gastric precancerous intestinal metaplasia and adenocarcinoma. J Infect Dis 2003;187:1165–77. [PubMed: 12695995]
13. O'Connell JT, Tomlinson JS, Roberts AA, et al. Pseudomyxoma peritonei is a disease of MUC2-expressing goblet cells. Am J Pathol 2002;161:551–64. [PubMed: 12163380]
14. O'Connell JT, Hacker CM, Barsky SH. MUC2 is a molecular marker for pseudomyxoma peritonei. Mod Pathol 2002;15:958–72. [PubMed: 12218214]
15. Li JD, Dohrman AF, Gallup M, et al. Transcriptional activation of mucin by Pseudomonas aeruginosa lipopolysaccharide in the pathogenesis of cystic fibrosis lung disease. Proc Natl Acad Sci USA 1997;94:967–72. [PubMed: 9023366]
16. Dohrman A, Miyata S, Gallup M, et al. Mucin gene (MUC 2 and MUC 5AC) upregulation by Gram-positive and Gram-negative bacteria. Biochim Biophys Acta 1998;1406:251–9. [PubMed: 9630659]
17. Souei-Mhiri M, Tlili-Graies K, Ben CL, et al. Mucocele of the appendix. Retrospective study of 10 cases. J Radiol 2001;82:463–8. [PubMed: 11353901]
18. Kuroki Y, Otagiri S, Tsukada K. Disseminated peritoneal adenomucinosis associated with a panperitonitis-like onset: report of a case. Surg Today 2001;31:646–50. [PubMed: 11495161]
19. Ronnett BM, Zahn CM, Kurman RJ, et al. Disseminated peritoneal adenomucinosis and peritoneal mucinous carcinomatosis. A clinicopathologic analysis of 109 cases with emphasis on distinguishing pathologic features, site of origin, prognosis, and relationship to "pseudomyxoma peritonei". Am J Surg Pathol 1995;19:1390–408. [PubMed: 7503361]
20. Tummuru MK, Cover TL, Blaser MJ. Cloning and expression of a high-molecular-mass major antigen of *Helicobacter pylori*: evidence of linkage to cytotoxin production. Infect Immun 1993;61:1799–809. [PubMed: 8478069]
21. Lan Z-D, Dai L, Zhuo X-L, et al. Gene cloning and sequencing of BmK AS and BmK AS-1, two novel neurotoxins from the scorpion *Butus martensi* Karsch. Toxicon 1999;37:815–23. [PubMed: 10219991]
22. Bendayan M, Nanci A, Kan FW. Effect of tissue processing on colloidal gold cytochemistry. J Histochem Cytochem 1987;35:983–96. [PubMed: 3302022]
23. Olivero OA, Chang PK, Lopez-Larraza DM, et al. Preferential formation and decreased removal of cisplatin-DNA adducts in Chinese hamster ovary cell mitochondrial DNA as compared to nuclear DNA. Mutat Res 1997;391:79–86. [PubMed: 9219551]
24. Semino-Mora C, Dalakas MC. Rimmed vacuoles with beta-amyloid and ubiquitinated filamentous deposits in the muscles of patients with long-standing denervation (postpoliomyelitis muscular atrophy): similarities with inclusion body myositis. Hum Pathol 1998;29:1128–33. [PubMed: 9781653]
25. Stirling JW, Graff PS. Antigen unmasking for immunoelectron microscopy: labeling is improved by treating with sodium ethoxide or sodium metaperiodate, then heating on retrieval medium. J Histochem Cytochem 1995;43:115–23. [PubMed: 7529784]
26. Aspholm M, Olfat FO, Norden J, et al. SabA Is the *H. pylori* hemagglutinin and is polymorphic in binding to sialylated glycans. PLoS Pathog 2006;2:989–1001.

27. Necchi V, Candusso ME, Tava F, et al. Intracellular, inter-cellular and stromal invasion of gastric mucosa, preneoplastic lesions, and cancer by *H. pylori*. Gastroenterology 2007;132:1009–23. [PubMed: 17383424]

28. Oliveira AG, Rocha GA, Rocha AM, et al. Isolation of *Helicobacter pylori* from the intestinal mucosa of patients with Crohn's disease. Helicobacter 2006;11:2–9. [PubMed: 16423084]

29. Thomas JE, Gibson GR, Darboe MK, et al. Isolation of *H. pylori* from human faeces. Lancet 1992;340:1194–5. [PubMed: 1359263]

30. Luzzi I, Covacci A, Censini S, et al. Detection of a vacuolating cytotoxin in stools from children with diarrhea. Clin Infect Dis 1996;23:101–6. [PubMed: 8816137]

31. Kang W, Rathinavelu S, Samuelson LC, et al. Interferon gamma induction of gastric mucous neck cell hypertrophy. Lab Invest 2005;85:702–15. [PubMed: 15765119]

32. Dabbagh K, Takeyama K, Lee HM, et al. IL-4 induces mucin gene expression and goblet cell metaplasia in vitro and in vivo. J Immunol 1999;162:6233–7. [PubMed: 10229869]

33. Kim YD, Kwon EJ, Park DW, et al. Interleukin-1beta induces MUC2 and MUC5AC synthesis through cyclooxygenase-2 in NCI-H292 cells. Mol Pharmacol 2002;62:1112–8. [PubMed: 12391274]

34. Thompson MA, Ashton RW, Pitot HC. Mucinous appendiceal adenocarcinoma presenting 5 years after appendectomy. Ann Intern Med 2004;140:E677–8.

35. Ohara N, Teramoto K. Successful treatment of pseudomyxoma peritonei with intraperitoneal 10 per cent dextrose, sizofiran and cisplatin. J Obstet Gynaecol 2002;22:223. [PubMed: 12521714]

36. Schistosomes, liver flukes and *Helicobacter pylori*. International Agency for Research on Cancer; Lyon, France: 1994. IARC Monograph on the evaluation of carcinogenic risks to humans. Anonymous

37. Itzkowitz SH, Yio X. Inflammation and cancer IV. Colorectal cancer in inflammatory bowel disease: the role of inflammation. Am J Physiol Gastrointest Liver Physiol 2004;287:G7–17. [PubMed: 15194558]

38. Kucharzik T, Maaser C, Lugering A, et al. Recent understanding of IBD pathogenesis: implications for future therapies. Inflamm Bowel Dis 2006;12:1068–83. [PubMed: 17075348]

39. Balish E, Warner T. *Enterococcus faecalis* induces inflammatory bowel disease in interleukin-10 knockout mice. Am J Pathol 2002;160:2253–7. [PubMed: 12057927]

40. Wang X, Huycke MM. Extracellular superoxide production by *Enterococcus faecalis* promotes chromosomal instability in mammalian cells. Gastroenterology 2007;132:551–61. [PubMed: 17258726]

41. Gatalica Z, Loggie B. COX-2 expression in pseudomyxoma peritonei. Cancer Lett 2006;244:86–90. [PubMed: 16427185]

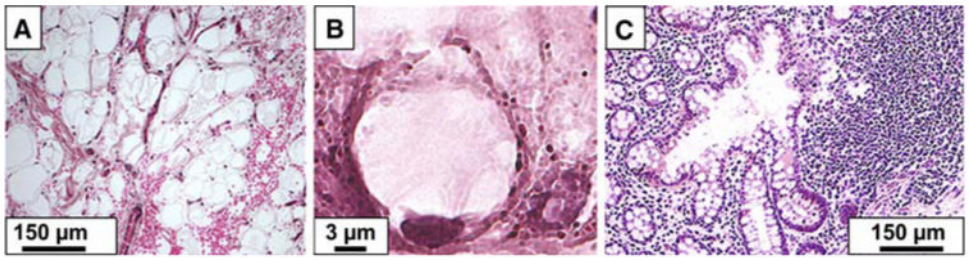

FIG. 1.

Multilobulated polypoid mucoid accumulation surrounded by the lamina propria, in the vicinity of lymphoid aggregate in a DPAM specimen **(A)**; one goblet cell containing mucin granules in a PMCA specimen **(B)**; glandular epithelia with mucosal hyperplasia associated with aggregates of lymphocytes, eosinophils and macrophages in a DPAM specimen **(C)**.

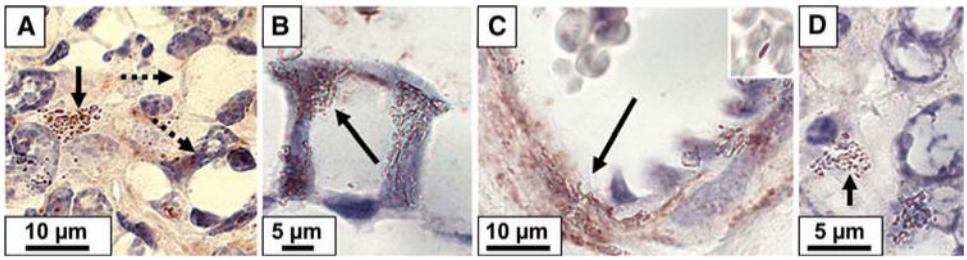

FIG. 2.

ISH detection of TNCB (arrows) in the vicinity of two cells typical of signet cell carcinoma (dashed arrows) **(A)**, in the cellular wall of goblet cell **(B)**, in the wall of capillaries and in close association with erythrocytes (insert) **(C)**, and inside inflammatory cell **(D)**.

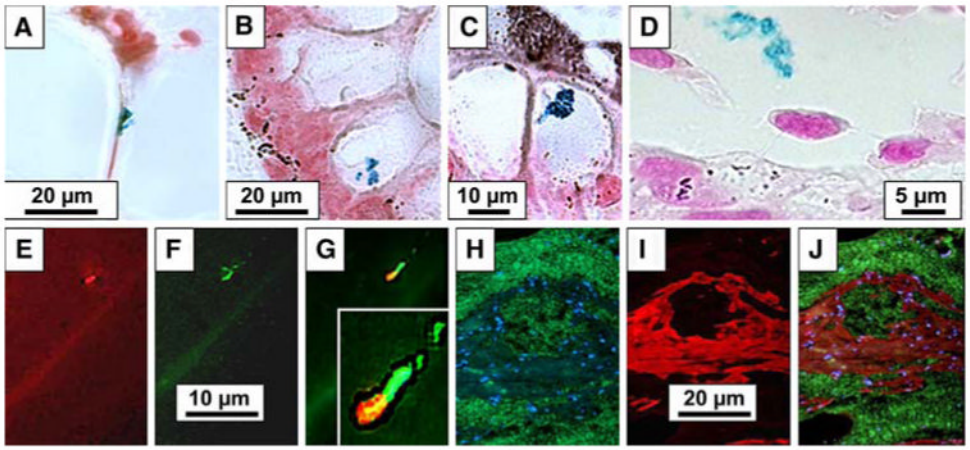

FIG. 3.

(A-D): ISH detection of *H. pylori 16S rRNA* expression (in blue) in the thin membrane limiting mucoid cavities **(A)**, inside the cytoplasm of columnar mucussecreting cell **(B)**, inside a goblet cell **(C)**, and in the lumen of a blood vessel **(D)**. **(E-G):** FISH detection of *H. pylori 16S rRNA* (**E**, red) and *cagA* (**F**, green) and co-localization of both **(G)**. Insert: Insert: higher magnification illustrating merged expression of *16S rRNA* (red) and *cagA* (green) in the core of *H. pylori* (yellow), with halo of *16S rRNA* expression (red, surrounding it), and *cagA* (green, at one end of the bacterium and extending onto flagelli. **(H-J)**: FISH detection of *MUC2* expression in mucoid deposits (green) and nuclei stained with dapi (blue) **(H)** and of *MUC5AC* expression (red), in the connective tissue containing mucoid accumulation **(I)**, with merge demonstrating separate expression of MUC5AC and MUC2 and the absence of co-localization (no yellow stain) **(J)**.

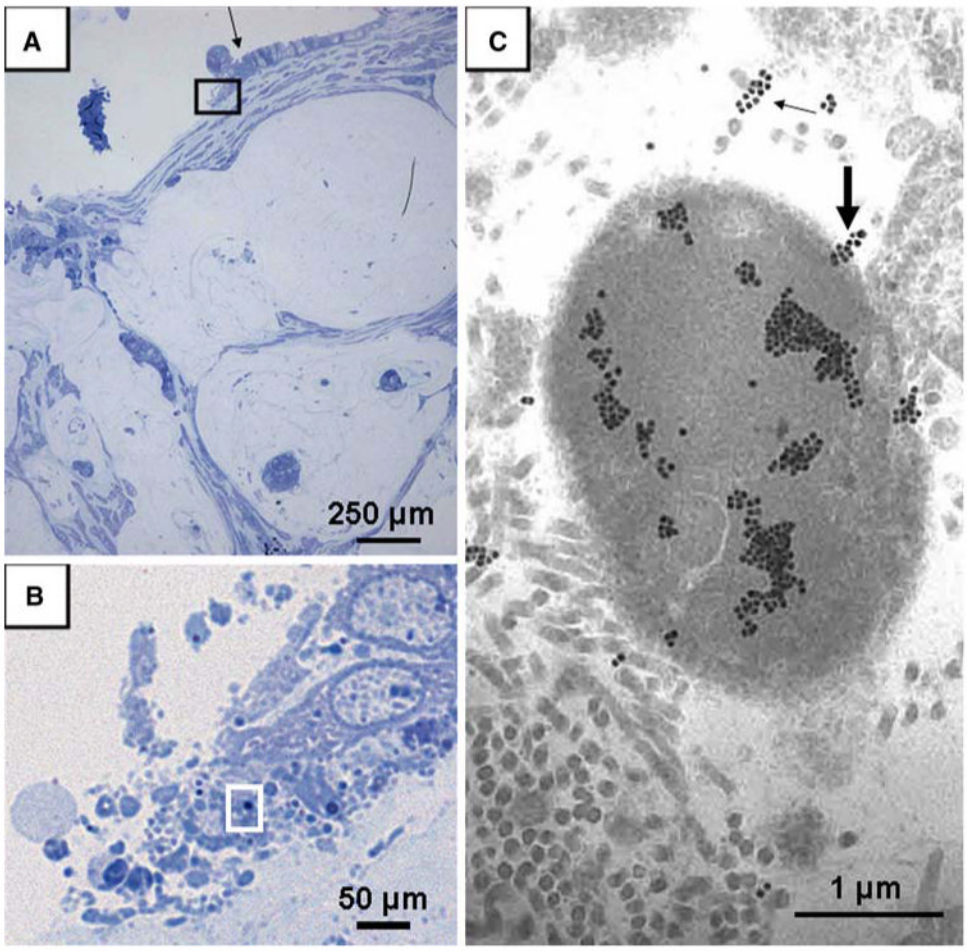

FIG. 4.

Semi-thin section photographed under light microscopy after toluidine blue staining and corresponding transmission electron microscopy picture. **(A)** pools of mucin with floating islands of malignant epithelium dissecting through the desmoplastic muscularis propria (100×) and columnar epithelial cells (black arrow) and luminal aggregates of bacteria. The area of the black rectangle in A is then observed under immersion (1000×) and illustrated in **B**, showing the morphology of columnar epithelial cells (black arrow in **A**) and the presence of luminal aggregates of bacteria. The area of the white rectangle in **B** is then observed in the next section under transmission electron microscopy and immunogold preparation and illustrated in **C**, showing a single *H. pylori* surrounded by cross, oblique, and longitudinal sections of connective tissue collagen fibrils. Most gold particles are localized in the homogeneous cytoplasmic portion (88%) but a few particles (12%) appear to label the emergence of a flagellum from the bacterium (thick arrow) or cross sections of flagellae (thin arrow).

TABLE 1

Bacterial density (N/10^6 μm^3) in the compartments of the PMP tissue. NNA: noninflamed, nonperforated, non-neoplastic appendix, N = 5; DPAM: disseminated peritoneal adenomucinosis, N = 6; PMCA: peritoneal mucinous carcinomatosis, N = 10

Bacterial type	Diagnosis	Epithelium	Lymphoid aggregates	Stroma	Free mucin
TNCB	NNA	48 ± 15	77 ± 12	68 ± 12	—
	DPAM	88 ± 19	72 ± 17	72 ± 11	169 ± 35
	PMCA	251 ± 64*	218 ± 38*†	266 ± 58*†	411 ± 111
H. pylori	NNA	10 ± 10	29 ±19	19 ± 19	—
	DPAM	24 ± 11	48 ± 13	40 ± 8	72 ± 17
	PMCA	72 ± 15*†	67 ± 16	59 ± 10	154 ± 36

TNCB, typed and noncultured bacteria. Values are means ± standard error on the mean (SEM).

* $p < 0.05$ versus NNA

† p standard < 0.05 versus DPAM.

Ann Surg Oncol. Author manuscript; available in PMC 2008 October 22.

TABLE 2

MUC2 and MUC5AC expression (in Vvi/10^4 μm) in the compartments of the PMP tissue. NNA: nonperforated, non-neoplastic appendix, N = 5; DPAM: disseminated peritoneal adenomucinosis, N = 6; PMCA: peritoneal mucinous carcinomatosis, N = 10

Apomucin	Diagnosis	Epithelium	Lymphoid aggregates	Stroma Vessels	Free mucin
MUC2	NNA	11 ± 8	41 ± 12	34 ± 4	—
	DPAM	264 ± 60	47 ± 16	31 ± 14	261 ± 51
	PMCA	356 ± 90*	170 ± 26*†	117 ± 25*†	1043 ± 282*
MUC5AC	NNA	335 ± 40	168 ± 26	134 ± 23	—
	DPAM	90 ± 13*	345 ± 20*	65 ± 17	37 ± 6
	PMCA	56 ± 12*	246 ± 17*	50 ± 15*	48 ± 9

Values are means ± SEM.

*$p < 0.05$ versus NNA

†$p < 0.05$ versus DPAM.